

## Modification of Indonesian Natural Zeolite (Clinoptillite-Mordenite) for Synthesis of Solketal

Dwi Kurniawati<sup>a</sup>, Jumaeri<sup>a</sup>, Silvester Tursiloadi<sup>b\*</sup>, Osi Arutanti<sup>b</sup>, Muhammad Safaat<sup>b</sup>

*a) Department of Chemistry, Faculty of Mathematics and Natural Sciences, Universitas Negeri Semarang Kampus Sekaran Gunungpati, 50229 Semarang, Indonesia*

*b) Research Center for Chemistry, National Research and Innovation Agency of the Republic of Indonesia, Kawasan PUSPIPTEK Serpong, Tangerang Selatan, 15314, Banten*

Received 7 April 2021; received in revised form 2 September 2021; accepted 24 September 2021

### ABSTRACT

Desilication of natural zeolite by alkali treatment to produce solketal was successfully prepared. Natural zeolite from Tasikmalaya, West Java, Indonesia, has been used as a catalyst source. The natural zeolite source was mordenite type structure. The experimental condition was varied to study their effect on the catalyst efficiency. Several characterization methods, such as Thermogravimetric Analysis (TGA), Brunauer Emmett Teller (BET), X-ray Diffraction (XRD), Scanning Electron microscopy (SEM), etc., were used to analyze the physicochemical properties of the prepared catalyst. From the temperature-programmed desorption of NH<sub>3</sub> (TPD analysis), the acidity of zeolite decreased from 0.597 to 0.444 by increasing NaOH concentration from 0.1 to 0.7 M, respectively. The result showed that alkali treatment did not change the phase structure of natural zeolite significantly. Here, the ratio of Si/Al decreased by increasing NaOH concentration, resulting in the decrease of acidity value. Interestingly, the efficiency of zeolite catalyst (HZ-01) shows the highest conversion and selectivity at around 98.73% and 74.66%, respectively. This exciting result opens the possibility to develop an economic catalyst with high efficiency from the abundant Indonesian mineral resource.

**Keywords:** Desilication, Glycerol, Natural zeolite, clinoptilolite, mordenite

### 1. Introduction

Fuel from vegetable oil and biomass has been developed as renewable energy and a substitute for fossil fuels. The Indonesian Palm Oil Producers Association (IPOA/GAPKI) is projecting the country's palm oil output to reach 49 million tons of Crude Palm Oil (CPO) in 2021. In Indonesia, the policy issues regarding palm oil and its waste as a substitute for fossil fuels have been issued by The Ministry of Energy and Mineral Resources with regulation No. 12/2015. Accordingly, palm oil and its derivatives as fuel have been widely developed, especially for biodiesel. However, the formation of side by-products from this process cannot avoid glycerol [1]. Therefore, how to utilize glycerol as a high-value chemical is an important concern.

The conversion of glycerol into high-value chemicals such as diglycerol isomer [2], glycerol carbonate [3], 2-phenyl-1,3-di-oxan-5-ol [4], 1,3-dioxolane [5], solketal [6] were developed and proposed. Among these derivative products, solketal, known as 4-hydroxymethyl-2,2-dimethyl-1,3-dioxolane, has a high potential as an additive to fuel due to its advantages. Because of its ability in enhancing the octane number, making solketal is believed to increase the ignitability and reduce the particle emissions [7-9]. Moreover, known as nontoxic solvents, suitable plasticizers, and suspending agents in pharmaceutical formulations [10] are other good potentials of solketal.

Manjunathan et al [11] showed that H-Beta has good performance as a catalyst for glycerol conversion into solketal. They showed that the 1:2 mole ratio of glycerol and acetone was the optimum condition that produced 86% and 98.5% of efficiency and selectivity, respectively. Sonar et al investigated that the conversion

\*Corresponding author:

E-mail address: [tursilo@gmail.com](mailto:tursilo@gmail.com) (S. Tursiloadi)

of carbonyl aldehyde to solketal was successfully achieved over hierarchical H/BEA catalyst [12]. Modified mordenite natural zeolite from Bayah by acid and heating treatment as the catalyst for ketalization has been studied by Nuryoto et al [13]. They were successful in converting glycerol up to 70% at 60°C. Unfortunately, the catalyst performance of zeolite, which has been treated by this method, is still low. Therefore, other treatments to improve the performance of natural zeolite are inevitable.

Some treatments of zeolite to improve the performance catalytic activity and other applications have been developed. In general, zeolites are three-dimensional aluminosilicates containing exchangeable cations that act as Lewis acid sites. Treatment of the natural zeolite with NaOH leads to the decreasing of silica content significantly, namely desilication [14]. By decreasing silica, zeolite will load more particles that causes an increase in catalytic activity [15]. Alkali treatment also increases the Na content by the formation of hydroxysodalite [16-18]. Furthermore, it shows that NaOH treatment alters the acidity of zeolite. Because of this phenomenon, alkali treatment of zeolite is believed to benefit the catalytic performance better than acid treatment. This comparison research was also proposed by previous researchers [19-21]. In addition, in the production of solketal, the presence of Lewis acid sites coordinates and activates the tertiary alcohol of the hemiketal.

Here, the modification of Indonesian natural zeolites by NaOH treatment is proposed to enhance the zeolite catalyst for glycerol conversion. The influence of reaction conditions such as reaction time, catalyst amount, and a molar ratio of acetone to glycerol was investigated to study their effect on the catalyzation of glycerol. The result showed that the alkali treatment process could enhance the conversion efficiency by almost 100%. Unlike the previous research, natural zeolite from Tasikmalaya, West Java, Indonesia has been used, showing that our Country has abundant mineral resources that can be used as an economic catalyst.

## 2. Experimental

### 2.1 Materials

The following materials have been used in this research: Natural zeolites from Tasikmalaya, West Java, Indonesia (PT. Gemilang Sejahtera Yasothama), NaOH (Merck), NH<sub>4</sub>Cl (Merck), AgNO<sub>3</sub> (Merck), glycerol (Merck), and acetone (Merck).

### 2.2 Catalyst Preparation

Twenty grams of natural zeolite (ZA) were dissolved in 400 mL NaOH under different Molar: 0.1 M, 0.3 M, 0.5 M, and 0.7 M, denoted HZ for treated-zeolite: HZ-0.1, HZ-0.3, HZ-0.5, and HZ-0.7, respectively. The mixture was stirred with a magnetic stirrer for 2 hours at 75°C, and then separated by using a vacuum filter. The next step was to rinse the prepared catalyst with H<sub>2</sub>O at pH 7 and dry at 110 °C for 12 hours. The prepared dry catalyst was then diluted into 150 mL of 0.1 M NH<sub>4</sub>Cl, heated under reflux at 80°C for 8 hours, and filtered. To remove the Cl<sup>-</sup> ions, the catalysts were rinsed in distilled water. For the last step, after drying at 110°C for 12 hours, the prepared catalyst was calcined at 500 °C for 4 hours. This method was referred to in the previous research [22-24].

### 2.3 Characterization

The thermogravimetric (TGA, Linseis STA PT 1600 analyzer) was used to analyze the natural zeolite's temperature decomposition. The crystal structure has been identified by X-ray diffraction (XRD, PW-1710 diffractometer Cu K $\alpha$  radiation at 40 kV and 30 mA, and a secondary graphite monochromator). A scanning electron microscope (SEM, Carl Zeiss AG, Jena, Germany) was used to determine the catalyst morphology. The Brunauer–Emmett–Teller (BET, Micromeritics TriStar II 3020 instrument) was used to calculate the specific surface area. The micropore surface area and micropore volume were evaluated using t-plot. The Barrett–Joyner–Halenda (BJH) method verified the pore size distributions from desorption branches. The temperature-programmed desorption of NH<sub>3</sub>(NH<sub>3</sub>-TPD, Tp-5080 Xianquan Industrial and Trading Co., Ltd, Tianjin, China) was applied to determine the strength of acid sites. Before NO<sub>3</sub>-TPD analysis, the prepared catalyst was degassed at 400 °C for 1 h followed by ammonia adsorption at 50°C. Next, the NH<sub>3</sub>-adsorbed zeolites were purged in N<sub>2</sub> flow gas for another 1h at 50°C to minimize NH<sub>3</sub> physisorption. Then, the TPD signals were recorded by heating the samples at a 10 °C/min rate in a helium flow to the target temperature (800°C). The total acidity or strength of the acid site was calculated by summarizing a weak acid and strong acid site.

### 2.4 Catalytic test

The prepared catalyst (0.5 – 3 %w) was diluted into 20 mL glycerol and acetone (1:2 mole) in a reflux reactor with a temperature condition of 60 °C at various reaction times, ranging from 2 to 8 hours. To obtain the solketal optimum yield, the mole ratio of glycerol/acetone was varied from 1:1 to 1:3. The main reaction products were

identified by gas chromatography-mass spectrometry analyses (GC-MS, Shimadzu MS-QP 2010 mass spectrometer instrument operating at 70 eV coupled with Shimadzu 2010 GC). The conversions and solketal yielding were calculated from calibration curves obtained with glycerol and solketal pure samples.

### 3. Results and Discussion

#### 3.1 Characterization of catalysts

TGA/DSC analysis result of natural zeolite is presented in **Fig. 1**. This analysis determines the weight characteristic of natural zeolite during the heating process. In general, the result reveals that a continuous weight loss procedure was observed for zeolite-treated alkaline.

The Figure has two distinct lines, i.e., a black line for TGA analysis and a red line for DSC analysis. For the black line, the decreasing weight in the temperature range from 50 to 200 °C was attributed to the weakly bond water and dehydration reaction. The loss of ignition is determined to be almost 8% mass, showing the water removal from the natural zeolite. The curve continuously decreased, suggesting that maximum dehydroxylation occurs at 700 °C. In the range of 300 to 500 °C, almost 15% mass was lost due to the decomposition of molecular and organic bonds [23,25]. It is known that the pores structures in the natural zeolite accommodate several cations. Accordingly, at the higher temperature (over 500 °C) during the TGA process, that not only increasing the water loss but also possibly causing the structure cracking resulted in the decreasing of zeolite size [26]. The DSC analysis result is presented in the red line showing the endothermic and exothermic effect resulting from energy consumption. The endothermic process occurred at 100 °C and over 700 °C, which was associated with weight loss. An exothermic reaction followed the endothermic reaction at 100 °C until it reached a peak temperature at 500 °C. This was due to the increase of water bond as the material dehydrates.

**Fig. 2** shows the N<sub>2</sub> adsorption and desorption from BET analysis results. The results showed that all of the prepared catalyst has the IV isotherm characteristics type revealed mesoporous structures. BJH analysis was also conducted to ensure detailed information of porous structure. The alkali treatment effect towards all prepared catalysts was summarized in **Table 1**.

The amount of NaOH influenced the characteristics of porous catalysts, although the amount of alkali did not change the SSA value significantly. The lowest SSA is

shown by ZA 12.911 m<sup>2</sup>g<sup>-1</sup> with the pore size at 19.75 nm. Alkali treatment succeeded in removing the impurities on the zeolite surface, enhancing the specific surface area. The most significant SBET value was shown by HZ-01 and HZ-07 of around 19 nm<sup>2</sup>g<sup>-1</sup> with the mesopore structures volume of 0.09 cm<sup>3</sup>g<sup>-1</sup>. In the case of HZ-03 and -05, mesoporous volume occurrence was due to the instability of the zeolite framework, and the structure quickly restructured during alkaline treatment. This result was also reported by Xiao et al. [23].

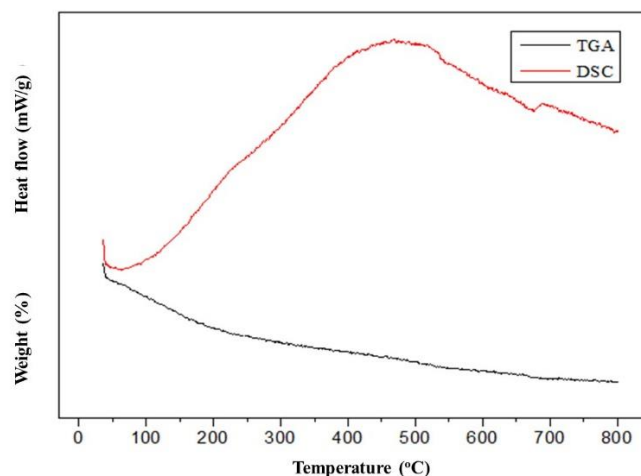


**Fig. 1.** TGA/DSC curve of a natural zeolite.

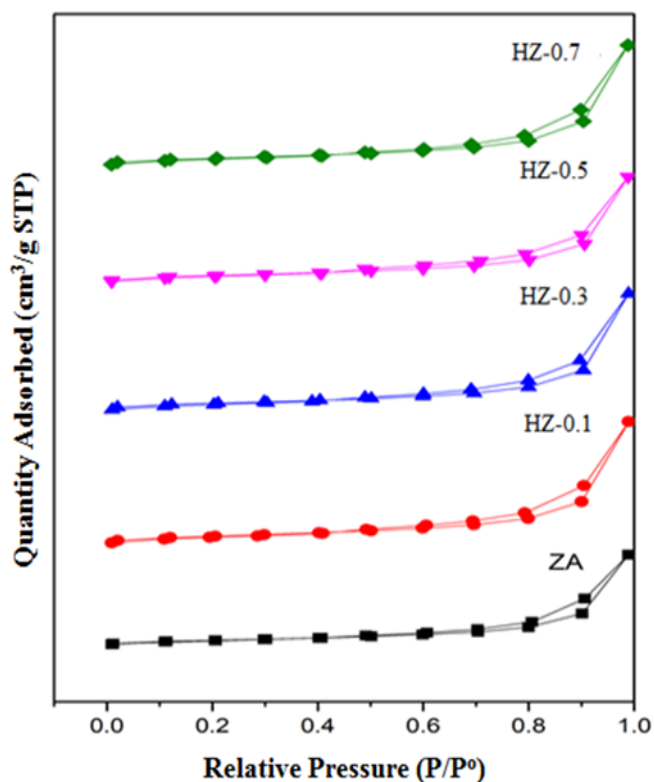


**Fig. 2.** N<sub>2</sub> adsorption and desorption isotherms before (ZA) and after alkali treatment (HZ 0.1 -0.7).

**Table 1.** Summary of BET and BJH analysis of zeolite catalysts

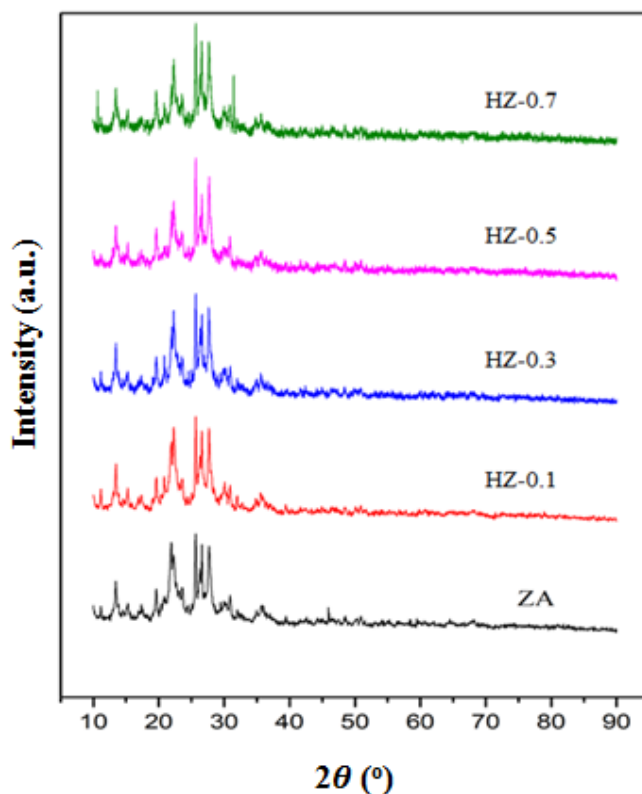
Sample	$S_{\text{BET}}$ ( $\text{m}^2 \cdot \text{g}^{-1}$ )	$V_{\text{total}}$ ( $\text{cm}^3 \cdot \text{g}^{-1}$ )	$V_{\text{micro}}$ ( $\text{cm}^3 \cdot \text{g}^{-1}$ )	$V_{\text{meso}}$ ( $\text{cm}^3 \cdot \text{g}^{-1}$ )	Pore Size (nm)
ZA	13.9112	0.0686	0.0004	0.0682	19.75
HZ-0.1	19.6636	0.0923	0.0003	0.0920	18.79
HZ-0.3	17.9379	0.0883	0.0008	0.0875	19.40
HZ-0.5	18.9384	0.0807	0.0013	0.0794	17.05
HZ-0.7	19.1115	0.0912	0.0008	0.0903	19.09

The XRD patterns of the prepared catalyst are presented in **Fig. 3**. All the XRD patterns exhibited similar peaks referred to JCPDS no. 73-1138 represent the mix of clinoptilolite and mordenite structure [27], with the main peak in the range of  $22^\circ$  to  $30^\circ$ . However, the dominant structure was mordenite, due to the peak of clinoptilolite after  $40^\circ$  could not be found. The different intensity of each peak (from  $20$  to  $25^\circ$ ) was due to the alkali treatment. However, the phase structure remained similar. The Scherrer equation has been used to evaluate the effect of alkali treatment on the zeolite crystallinity by measuring the highest peak ( $2\theta = 26^\circ$ ) for each sample [28-31]. Besides the difference in peak intensity, the number of alkalis also did not influence the crystallinity ominously. The crystal size of ZA without alkali treatment was around 39 nm. By increasing the concentration of alkali, the crystallite size of alkali increased up to 50 nm. Based on the XRD analysis results, it can be inferred that alkali treatment will enhance the crystallinity and some of the peaks of zeolite due to the removal of impurities.

The effect of alkali treatment was thought to affect the zeolite morphology. Scanning electron microscopy was conducted to analyze the zeolite morphology with results shown in **Fig. 4**. In general, the morphology of natural zeolite before and after alkali treatment was very similar. **Fig. 4a** shows the natural zeolite before alkali treatment as a reference. Some small particles were distributed on the zeolite surface, indicating the possible presence of impurities. **Fig. 4b-4e** shows the treated zeolite under various alkali concentrations. Compared to **Fig. 4a**, the surface morphology of treated zeolite is clearer. To determine the effect of alkali treatment on the zeolite composition, EDX analysis has been conducted. The summary of EDX analysis is shown in **Table 2**. The result shows that all-natural zeolite contained Silica (Si) and Aluminum (Al) as a basic element of zeolite [32-34]. However, the alkali

treatment decreased the ratio of Si/Al concentration. This phenomenon occurred because at the higher NaOH concentration, the Si atom was more easily extracted than the Al atom, called desilication. A similar phenomenon was also reported by Akgul et al. [35].

**Fig. 5** shows the TPD-NH<sub>3</sub> profiles of the pure- (ZA) and treated-zeolite (HZ-). In general, all the prepared zeolites have two desorption peaks. At the low-temperature peak range ( $100$ - $400^\circ\text{C}$ ), the peak corresponds to NH<sub>3</sub> adsorbed on non-acidic -OH groups and NH<sup>4+</sup>. On the other hand, a higher temperature range

**Fig. 3.** X-ray diffraction pattern of the natural zeolite, before (ZA) and after alkali treatment (HZ 01-07).

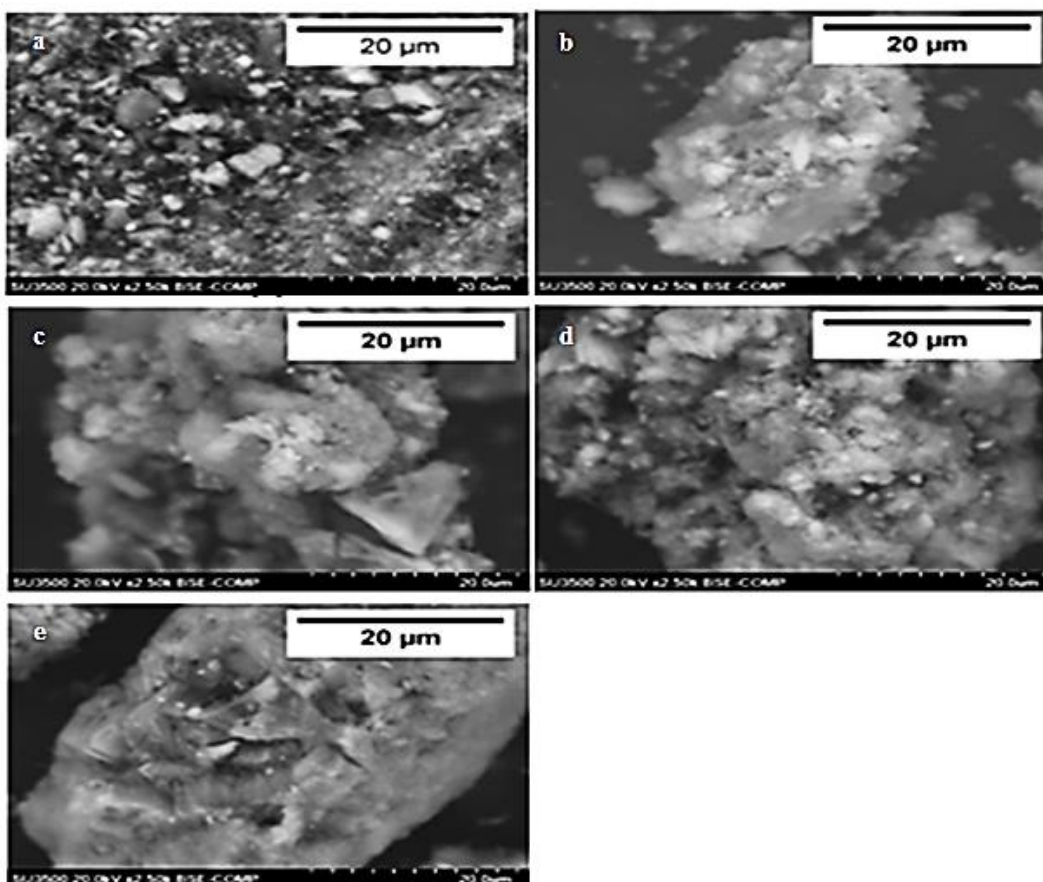


**Fig. 4.** SEM micrographs of (a) ZA (b) HZ- 0.1 (c) HZ-0.3 (d) HZ-0.5 (e) HZ-0.7

**Table 2.** Si/Al ratio of natural zeolite before and after treatment

Sample	Si/Al Ratio
ZA	5.15
HZ-0.1	5.02
HZ-0.3	4.80
HZ-0.5	4.43
HZ-0.7	4.33

(500-600°C) corresponds to  $\text{NH}_3$  adsorbed on authentic acid sites. The HZ-01 showed the highest peaks, showing that alkali treatment influences the acidity of treated zeolite.

The summary of zeolite surface acidity as the effect of alkali treatment is shown in **Table 3**. The analysis was conducted by TPD analysis.

The result showed that the acidity of the treated zeolite decreased by increasing the concentration of NaOH, indicating dealumination occurred during the alkali treatment. This result was similar to that in **Table 2**, where the alkali treatment was causing the decreasing of Al atom on the zeolite. Therefore, based on the specific surface area and total acidity, the HZ-01 catalyst was the best catalyst for synthesizing solketal. Here, the Si/Al

ratio in the alkaline-treated zeolite was lower than that of the natural zeolite. This number influenced the number of potential Brønsted acid sites per unit weight, providing the configuration of aluminum tetrahedral [36-38].

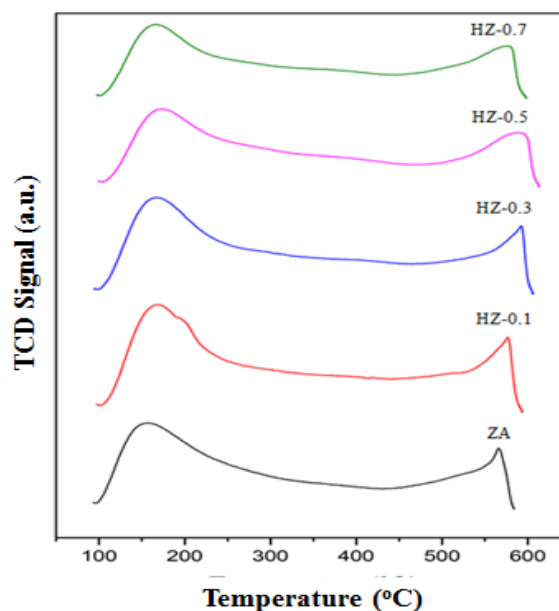


**Fig. 5.** TPD- $\text{NH}_3$  graph on natural zeolites

**Table 3.** Total acidity data of natural zeolite catalysts

Sample	Total acidity (mmol/g)
ZA	0.5385
HZ-0.1	0.5968
HZ-0.3	0.5805
HZ-0.5	0.4288
HZ-0.7	0.4439

### 3.2 Catalytic Activity

The catalyst activity test was carried out using reflux with variations in the mole ratio of glycerol and acetone (1:1, 1:2, and 1:3), varied reaction times of 2, 5, and 8 hours, and catalyst concentrations of 0.5, 1, and 3%. The effect of variations in the mole ratio of glycerol and acetone in the catalyzed reaction to solketal using natural zeolites for 2 hours, at a catalyst concentration of 1% and a temperature of 60°C is presented in **Fig. 6**.

Effect of reaction time on the ketalization reaction using HZ-01 catalyst are 2, 5, and 8 hours with a reactant ratio of 1:2, at 60°C and a catalyst concentration of 1% are presented in **Fig. 7**. At 5 hours, the highest glycerol conversion and solketal selectivity were 98.73% and 74.6% respectively. The low reaction time was encouraging the increase of kinetic reaction causing the exothermic reaction to occur. By increasing the reaction time gradually, the kinetic reaction increased to reach the equilibrium yield. After reaching the equilibrium point, the conversion and selectivity decreased even though the reaction time still increased. Unfortunately, the solketal selectivity only reached 74.7%, much lower compared to conversion efficiency. It was probably due to the low boiling point of acetone (56°C), making the number of acetone was not sufficient to solketal selectivity until 100%. A similar phenomenon was also proposed by previous research [39,40].

The effect of various catalyst concentrations on glycerol conversion and solketal selectivity is shown in **Fig.8**. The system was set under a reactant ratio of 1:2 and reaction temperature at 60°C for 5 hours. The result showed that by increasing the catalyst ratio from 0.5 to 1.0 %w, the glycerol conversion increased from 80 to 100%, and solketal selectivity increased from 60 to 75%, respectively. Thus, the enhancement of conversion and selectivity phenomenon was caused by the active site area of the catalyst that interacted with the acetone directly. However, the exceeding amount of catalyst resulted in a decrease in both glycerol conversion and solketal selectivity. In addition, because of a large number of catalysts, the catalyst will agglomerate and reduce the interaction space. In other

words, the catalyst's active site decreased, weakening conversion and selectivity ability. In general, the catalyst reaction between the zeolite structure to glycerol conversion and solketal selectivity was proposed as follows. First, glycerol and acetone interact, forming a hemiketal (3-(2-hydroxypropan-2-yl)oxy)propane-1,2-diol) for the first step. This process was followed by a carbenium ion that is stabilized and activated for a nucleophilic attack from one of the alcoholic groups of glycerol, leading to the formation of solketal or the six-membered ring ketal (2,2-dimethyl-1,3-dioxan-5-ol). This process was dependent on Brønsted acid sites or Lewis acid sites [9,40-42]. The presence of Lewis acid sites coordinates and activates the tertiary alcohol of the hemiketal. For the final step, the intramolecular reaction with one of the alcoholic groups leads to the formation of solketal and the isomer.

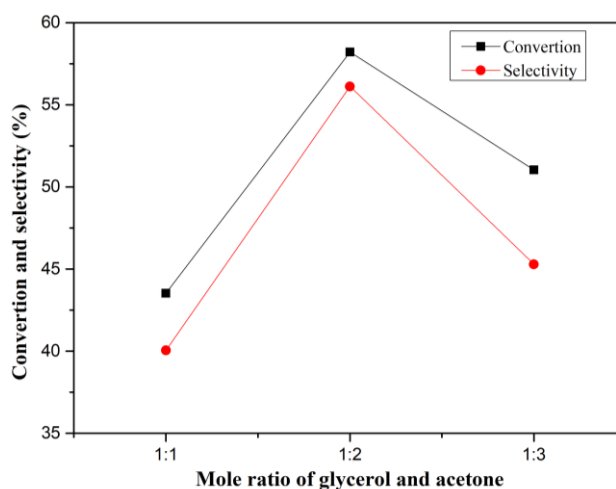


**Fig. 6.** Effect of the mole ratio of glycerol and acetone on glycerol conversion and solketal selectivity.

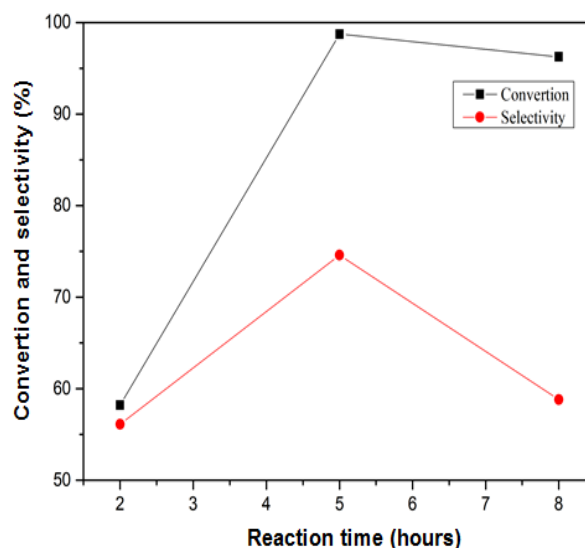


**Fig. 7.** Effect of reaction time on glycerol conversion and solketal selectivity

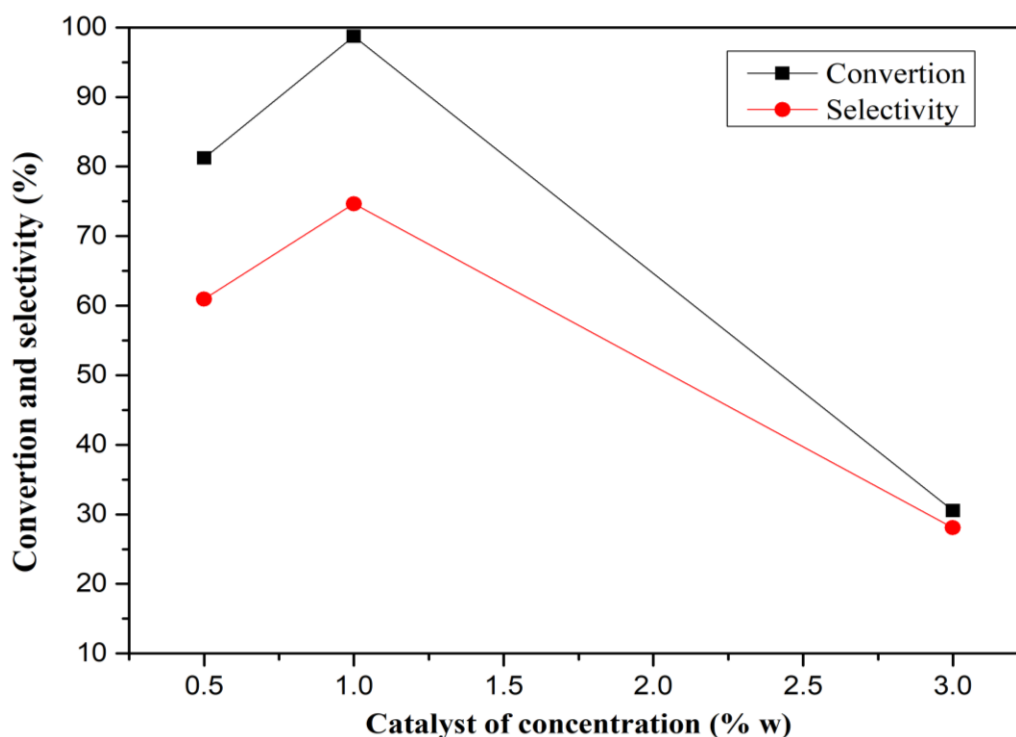


**Fig. 8.** Effect of catalysts concentration on glycerol conversion and solketal selectivity

**Table 4.** Summarized of comparison result studies

Catalysts	Ratio (Gly : Ace)	%Catalysts (%w)	Reaction time (hour)	Conversion (%)	References
p-toluenesulfonic acid	1:6	1	12	82.7	[43]
FeCl <sub>3</sub> (1-NO <sub>2</sub> )	1:4	1.39	0.16	92	[44]
Fe(NO <sub>3</sub> ) <sub>3</sub> .9H <sub>2</sub> O	1:20	0.3	0.16	100	[41]
Zr-S-600	1:6	0,6	0.16	88	[9]
[Eu <sub>2</sub> (H <sub>4</sub> nmp) <sub>2</sub> (H <sub>2</sub> O) <sub>2</sub> (SO <sub>4</sub> )]·H <sub>2</sub> O	1:10	5	6	84	[45]
H-BEA	1:4	5	3	85	[46]
Current result (natural zeolite)	1:2	1	5	98.73	

Comparison results between the current result with previous research have been proposed in **Table 4**. The result showed that the current catalyst has almost the highest efficiency in conversion glycerol, where the catalyst mass and reaction time was relatively low.

#### 4. Conclusions

Desilication of natural zeolites of Tasikmalaya, West Java, Indonesia, has been successfully prepared by alkali treatment. The characteristics of natural zeolite were significantly different after the treatment. By increasing the alkali concentration, the crystallinity of zeolite increased up to 50 nm due to the removal of impurities. Meanwhile, the specific surface area and acidity decreased. The condition affected the yield of

solketal and glycerol conversion. The optimum ratio of acetone concentration resulted in the highest efficiency conversion and selectivity of around 98.73% and 74.66%, respectively. This interesting research result provides good information related to the utilization of natural zeolite from Indonesia for a promising catalyst.

#### Acknowledgements

We gratefully acknowledge the financial support given for this work by the research fund of Deputy for Engineering Sciences, Indonesian Institute of Sciences. This research was carried out with the analytical services provided thanks to financial support of PPII LIPI in the framework of E-Layanan Sains Program.

## References

- [1] C.G. Chol, R. Dhabhai, A.K. Dalai, M. Reaney, Fuel Process. Technol. 178 (2018) 78–87.
- [2] M. Ayoub, A.Z. Abdullah, Chem. Eng. J. 225 (2013) 784–789.
- [3] M. Manikandan, P. Sangeetha, Chem. Select 4 (2019) 6672–6678.
- [4] K. Yamamoto, A. M. Kiyon, J. C. Bagio, K. A. B. Rossi, F. D. Berezuk, M. E. Berezuk, Green Process Synth. 8 (2019) 183–190.
- [5] R.M. Kulkarni, N. Arvind, Holiyon 7 (2021) e06018
- [6] K. Stawicka, A.E. Díaz-Álvarez, V. Calvino-Casilda, M. Trejda, M.A. Bañares, M. Ziolek, J. Phys. Chem. C 120 (2016) 16699–16711.
- [7] W. Xiong, Z. Yu-hua, L. Cheng-chao, H. Jing-ping, W. Liang, C. Yao, L. Jin-lin, J. Fuel Chem. Technol. 45 (2017) 950-955.
- [8] M.N. Moreira, R.P.V. Faria, A.M. Ribeiro, A.E. Rodrigues, Ind. Eng. Chem. Res. 58 (2019) 17746-17759.
- [9] J.A. Vannucci, N.N. Nichio, F. Pompeo, Catal. Today (2020)
- [10] J.C. Groen, J.A. Moulijn, J. Pérez-Ramírez, Microporous Mesoporous Mater. 87 (2005) 153-161.
- [11] P. Manjunathan, S.P. Maradur, A.B. Halgeri, V.S. Ganapati, J. Mol. Catal. A:Chem. 396 (2015) 47-54.
- [12] S.K. Sonar, A.S. Shinde, P.S. Niphadkar, S. Mayadevi, P.N. Joshi, V.V. Bokade, Environ. Prog. Sustainable Energy 37 (2017) 797-807.
- [13] N. Nuryoto, H. Sulistyono, W.B. Sediawan, I. Perdana, Reaktor 16 (2016) 72-80.
- [14] G. Hu, J. Yang, X. Duan, R. Farnood, C. Yang, J. Yang, W. Liu, Q. Liu, Chem. Eng. J. 417 (2021) 129209-129227.
- [15] A. Nezamzadeh-Ejhi, M. Khorsandi, J. Hazard. Mater. 176 (2010) 629-637.
- [16] A. Ates, J. Colloid Interface Sci. 523 (2018) 266-281.
- [17] Y. He, S. Tang, S. Yin, S. Li, Journal of Cleaner Production 306 (2021) 127248-127265.
- [18] T. Tamiji, A. Nezamzadeh-Ejhi, J. Solid State Electrochem. 23 (2019) 143–157
- [19] Y. Wang, T. Yokoi, S. Namba, T. Tatsumi, Catalysts 6 (2016) 1–19.
- [20] Z.V. Rahbari, M. Khosravan, A.N. Kharat, Iran. J. Catal. 7(3) (2017) 217-223.
- [21] A. Khaleque, M. M. Alam, M. Hoque, S. Mondal, J. B. Haider, B. Xu, M.A.H. Jahir, A.K. Karmakar, J.L. Zhou, M. B. Ahmed, M.A. Moni, Environmental Advances 2 (2020) 100019-100042.
- [22] R.A. Fauzi, S. Tursiloadi, A.A. Dwiarmoko, D. Sukandar, F. Aulia, N. Rinaldi, Sudiarmanto, Jurnal Kimia Valensi 5 (2019) 236-241.
- [23] W. Xiao, F. Wang, G. Xiao, RSC Advances 5 (2015) 1–8.
- [24] S. Chassaing, V. Bénateau, P. Pale, Current Opinion in Green and Sustainable Chemistry 10 (2018) 35-39
- [25] A. Nezamzadeh-Ejhi, S. Tavakoli-Ghinani, Comptes Rendus Chimie, 17 (2014) 49-61
- [26] R. J. Argauer, M.D. Kensington, G. R. Landolt, N.J. Audubon, U.S. Patent No. 3702886, Mobil Co. (1972).
- [27] M.M.J. Treacy, J.B. Higgins, Elsevier Science 485 (2007) 182-243.
- [28] N. Pourshirband, A. Nezamzadeh-Ejhi, S.N. Mirsattari, Chem. Phys. Lett. 761 (2020) 138090
- [29] M. Balakrishnan, R. John, Iran. J. Catal. 10 (2020) 1-16
- [30] T. Tamiji, A. Nezamzadeh-Ejhi, J. Taiwan Institute Chem. Eng. 104 (2019) 130-138
- [31] T. Tamiji, A. Nezamzadeh-Ejhi, J. Electroanal. Chem. 829 (2018) 95–105
- [32] M. Reháková, S. Cuvanová, M. Dzivák, J. Rimár, Z. Gaval'ova, Curr. Opin. Solid State Mater. Sci. 8 (2004) 397–404.
- [33] R. Saab, K. Polychronopoulou, L. Zheng, S. Kumar, A. Schiffer, J. Ind. Eng. Chem. 89 (2020) 83-103
- [34] C. Feng, J. E. W. Han, Y. Deng, B. Zhang, X. Zhao, D. Han, Renew. Sustain. Energy Rev. 144 (2021) 110954-110980.
- [35] M. Akgul, A. Karabakan, Microporous Mesoporous Mater. 145 (2011) 157-164.
- [36] M. Ravi, V.L. Sushkevich, J.A. van Bokhoven, Chem. Sci. 12 (2021) 4094-4103.
- [37] S. Rostami, S.N. Azizi, F. Rigi, Iran. J. Catal. 7(4) (2017) 267-276.
- [38] T.T. Le, A. Chawla, J.D. Rimer, J. Catal. 391 (2020) 56-68
- [39] M.R. Nanda, Z. Yuan, W. Qin, H.S. Ghaziaskar, M.A. Poirier, C.C. Xu, Fuel 117 (2014) 470-477.
- [40] M.R. Nanda, Y. Zhang, Z. Yuan, W. Qin, H.S. Ghaziaskar, C. Xu, Renew. Sustain. Energy Rev. 56 (2016) 1022-1031.
- [41] M.J. da Silva, A.A. Rodrigues, P. F. Pinheiro, Fuel, 276 (2020) 118164-118171.
- [42] R. Bai, Y. Song, Y. Li, J. Yu, Trends Chem. 1 (2019) 601-611
- [43] Suriyapradiloka, B. Kitiyanan. Energy Procedia 9 (2011) 63 – 69.
- [44] F. Taddeo, R. Esposito, V. Russo, M. Di Serio, Catalysts 11 (2021) 83-94.
- [45] I.C.M.S. Santos-Vieira, R.F. Mendes, F.A.A. Paz, J. Rocha, M.M.Q. Simões, Catalysts 11 (2021) 598-611.
- [46] V. Rossa, G.C. Díaz, G.J. Muchave, D.A.G. Aranda, S.B.C. Pergher, Glycerine Production and Transformation - An Innovative Platform for Sustainable Biorefinery and Energy (2019)